Assessing Interannual Variability in Marginal Ice Zones

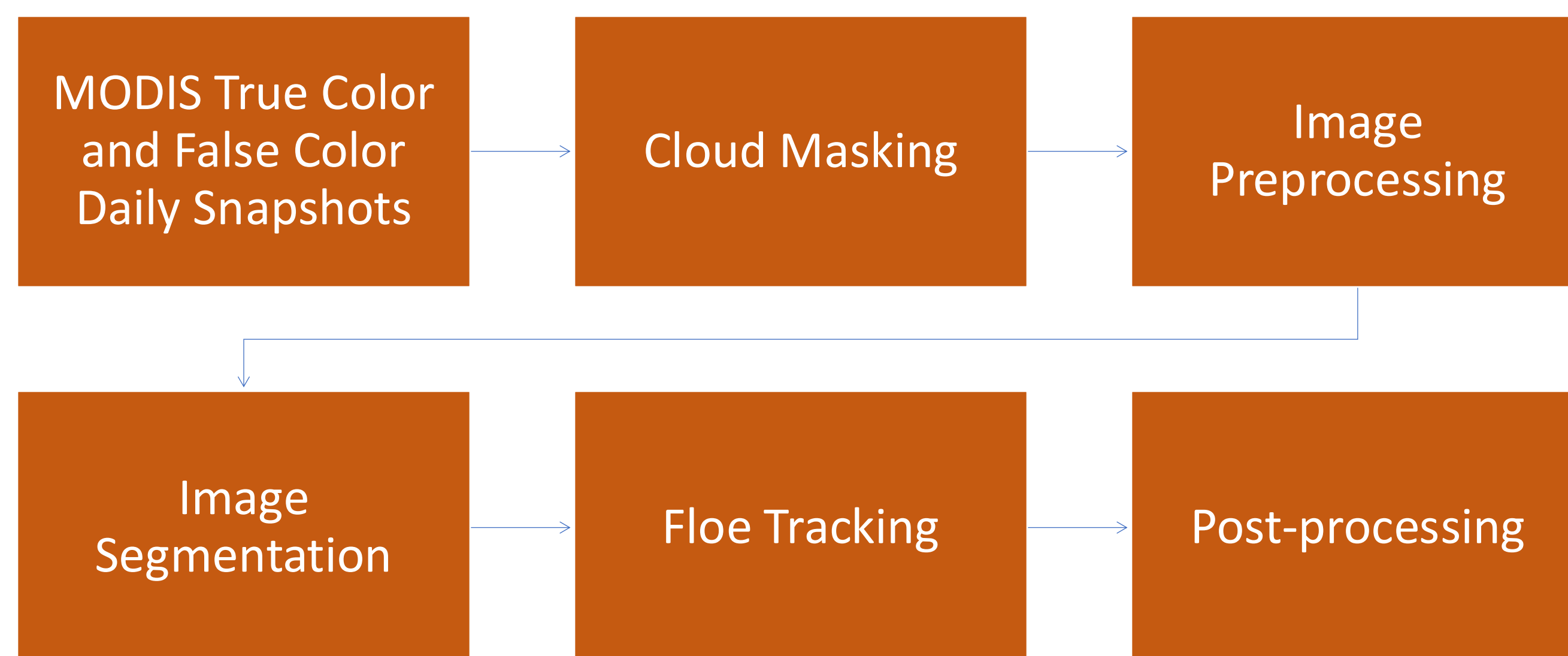[1]Daniel M. Watkins, [2]Jennifer K. Hutchings, [1]Monica M. Wilhelmus
[1]Center for Fluid Mechanics, Brown University, Providence, RI
[2]College of Earth, Ocean, and Atmospheric Science, Oregon State University, Corvallis, OR

School of Engineering — BROWN UNIVERSITY

Background Sea ice motion in marginal ice zones (MIZs, where sea ice is impacted by ocean waves) is complex. Ice drift in MIZs is highly variable interannually and seasonally and thus is challenging to characterize with standard observations and models [1]. The size of individual pieces of ice—the floe scale—determines the relationship between sea ice and the scales of motion of the atmosphere and ocean [2, 3]. However, standard in situ and remote sensing ice observations calculate ice motion and floe shape properties separately. Previous work using the Ice Floe Tracker (IFT) algorithm [4] has leveraged long-term observations from NASA's Moderate Resolution Imaging Spectroradiometer (MODIS) to jointly observe ice floe shapes and dynamics, measuring interannual variability in Beaufort Sea upper ocean energetics [5] and East Greenland ice dynamics [6, 7].
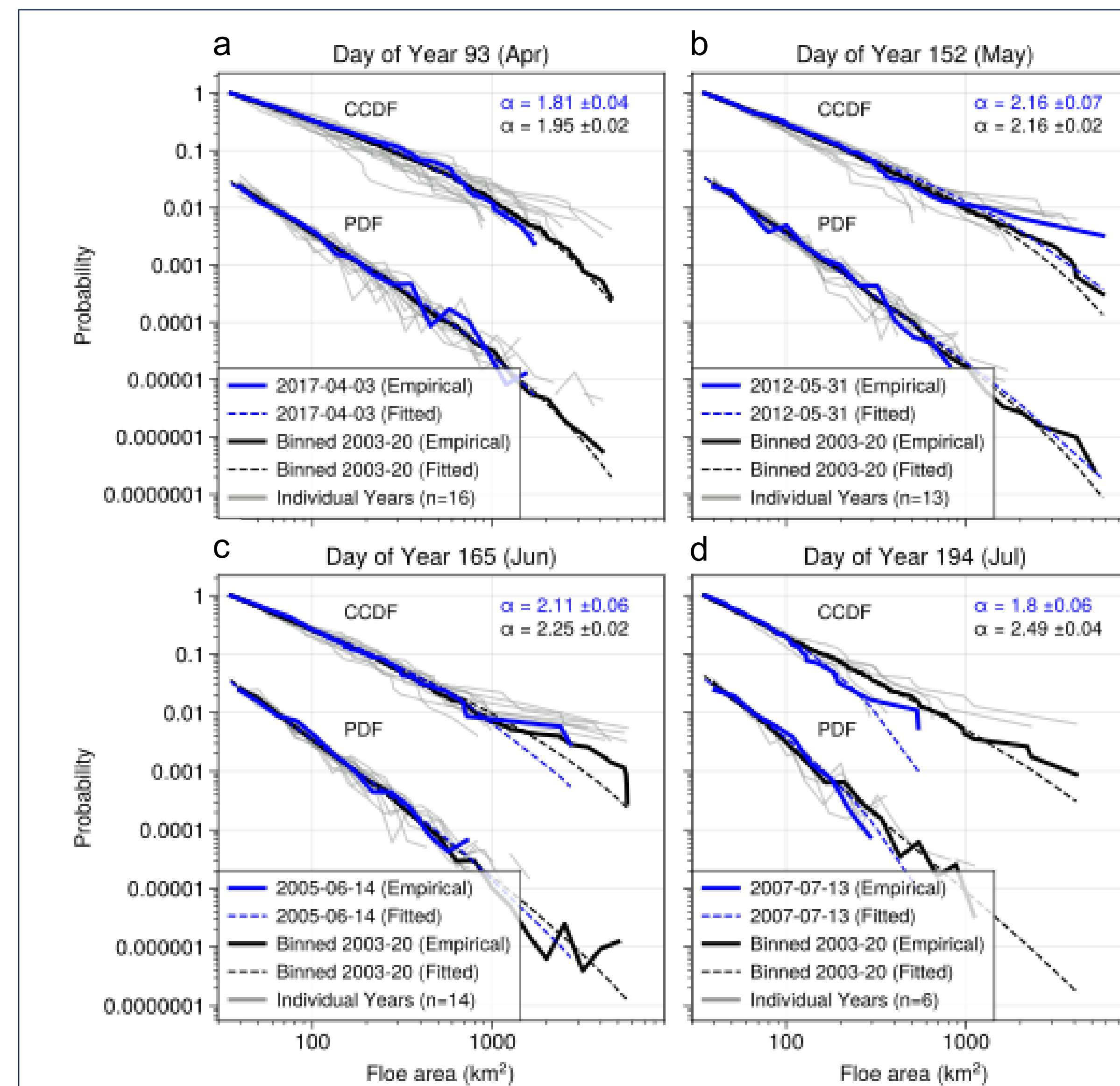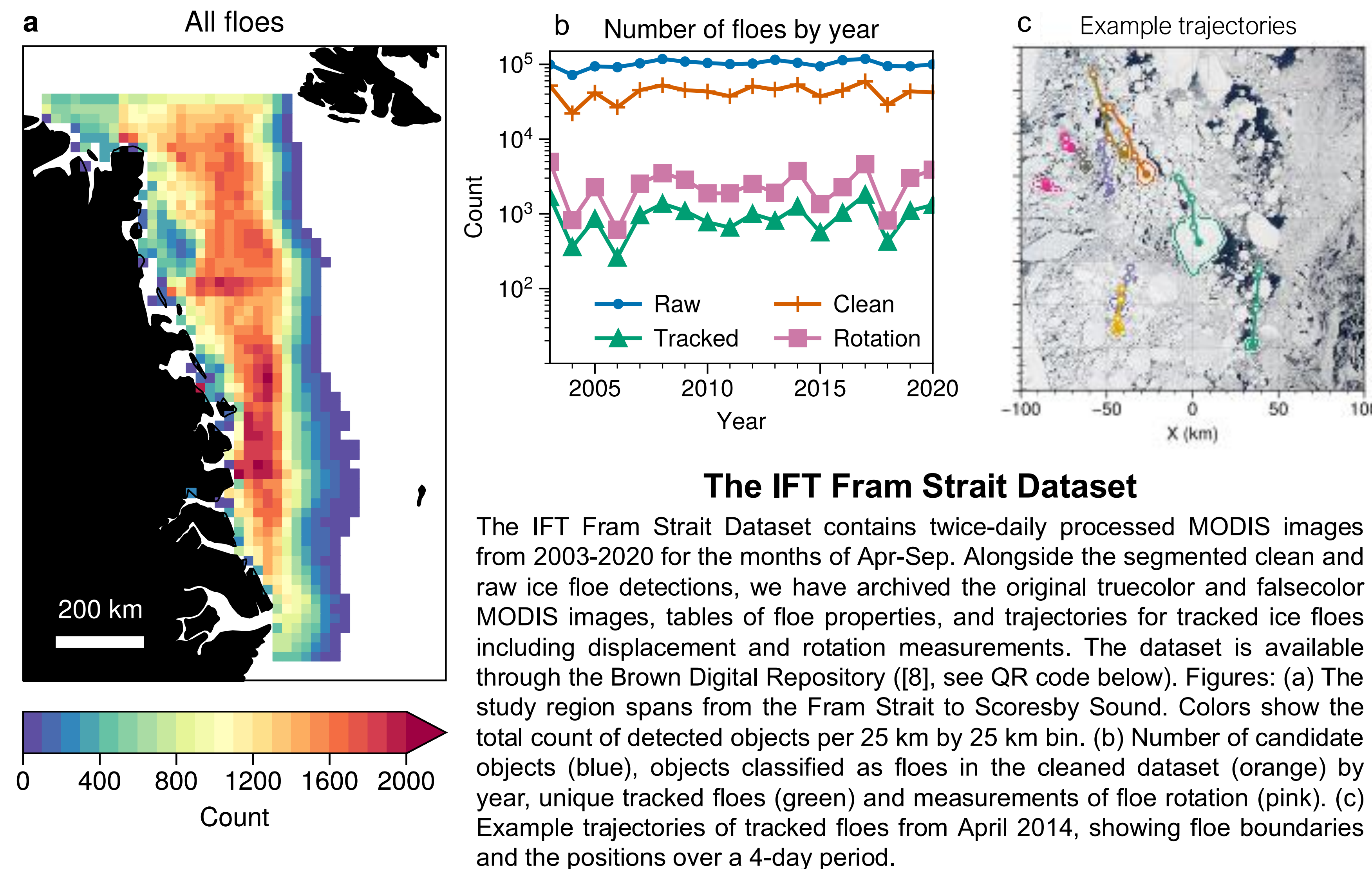
Results A new version of the IFT ice segmentation and tracking dataset enables analysis of the floe size distribution (FSD) alongside floe-scale motion and rotation for the Fram Strait and Greenland Sea region [14]. We find:

- The FSD is best approximated by a parametric fit to an exponentially truncated power law distribution
- The slope of the FSD displays distinct seasonality with substantial interannual variability
- The number of detected floes consistently increases near the beginning of June, coincident with landfast ice breakup

The Ice Floe Tracker (IFT) Algorithm

MODIS True Color and False Color Daily Snapshots → Cloud Masking → Image Preprocessing → Image Segmentation → Floe Tracking → Post-processing

- **Data** Daily mid-day near-real-time MODIS images from the *Aqua* and *Terra* satellites, color-corrected, calibrated reflectance "true color" (bands 1-4-3) and "false color" (bands 7-2-1). We obtain satellite overpass time using the Satellite Overpass Information Tool (SOIT) [9].
- **Masking and pre-processing** The IFT cloud mask covers only thick clouds, allowing ice floes under thin clouds to be identified. Pre-processing steps include sharpening, histogram adjustment, morphological operations, normalization, and binarization.
- **Segmentation** We apply multiple segmentation routines including k-means and watershed functions, and include two similar segmentation pipelines. Candidate floes identified in both pipelines are retained.
- **Tracking** Floe tracking is based on pairwise comparison of shape statistics, including geometric measures, correlation between boundary curves, and area disagreement after rotation.
- **Post-processing** Shape features and mean reflectance of tracked floes are used to train a logistic regression classifier, which we use screen non-tracked candidate floes. Including non-tracked quality-controlled floes increases the number of floes available for FSD analysis by more than an order of magnitude.
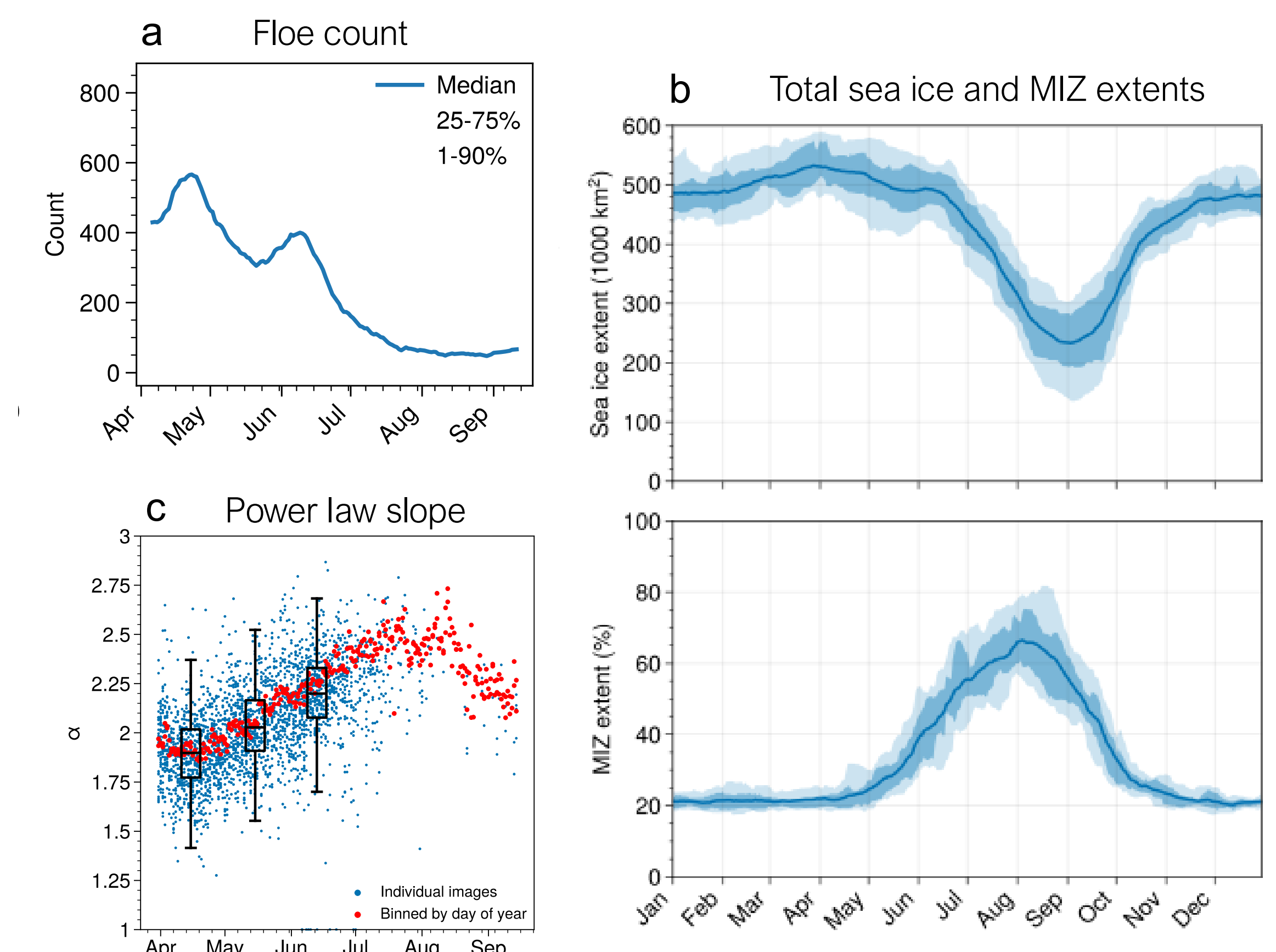
The IFT Fram Strait Dataset

a All floes **b** Number of floes by year **c** Example trajectories

Raw · Clean · Tracked · Rotation

The IFT Fram Strait Dataset contains twice-daily processed MODIS images from 2003-2020 for the months of Apr-Sep. Alongside the segmented clean and raw ice floe detections, we have archived the original truecolor and falsecolor MODIS images, tables of floe properties, and trajectories for tracked ice floes including displacement and rotation measurements. The dataset is available through the Brown Digital Repository ([8], see QR code below). Figures: (a) The study region spans from the Fram Strait to Scoresby Sound. Colors show the total count of detected objects per 25 km by 25 km bin. (b) Number of candidate objects (blue), objects classified as floes in the cleaned dataset (orange) by year, unique tracked floes (green) and measurements of floe rotation (pink). (c) Example trajectories of tracked floes from April 2014, showing floe boundaries and the positions over a 4-day period.

Characterizing the FSD

a Day of Year 93 (Apr) **b** Day of Year 152 (May) **c** Day of Year 165 (Jun) **d** Day of Year 194 (Jul)

a: α = 1.81 ±0.04, α = 1.95 ±0.02
b: α = 2.16 ±0.07, α = 2.16 ±0.02
c: α = 2.11 ±0.06, α = 2.25 ±0.02
d: α = 1.8 ±0.06, α = 2.49 ±0.04

The range and frequency of floe sizes is summarized by the FSD. The probability density function (PDF) of the FSD is often nearly linear in log-log space. Hence it is often summarized by a simple power-law fit:

$$p(x) \sim x^{-\alpha}$$

The parameter α is the power-law slope. Observations show that (1) is not always a good fit [9, 10]. Following [11, 12] we used log-likelihood ratios to evaluate the power law vs. the lognormal distribution and the truncated power law, given by

$$p(x) \sim x^{-\alpha}e^{-\lambda x}$$

Both the lognormal and truncated power law distributions have higher likelihood ratios than the standard power law. The truncated power law has higher likelihood than the lognormal distribution for the first part of the year (Apr-Jun), while the two distributions are equally likely after July.

Interannual variability of the FSD. The FSD for 4 randomly selected days of year (DOY). Single year in blue, other years on the same DOY in gray, and binned across all years for the same DOY in black. Empirical estimates of the probability density function (PDF) and the complimentary cumulative distribution function (CCDF) are solid; best fit with dashed lines.

Seasonality and interannual variability in the MIZ

The sea ice cover varies strongly in space and time. Observations of sea ice floe shapes from the IFT complement observations from standard long-term datasets such as passive microwave estimates of sea ice concentration, offering an additional angle to track seasonal and interannual variability. In the Greenland Sea, the sea ice extent reaches its maximum in late March, then decreases only slightly until mid June. Thereafter the ice extent decreases sharply until the minimum in early September. The percentage of that ice cover in the MIZ (using the concentration-based definition) increases from 20% in May to over 60% in August. The IFT observations show that the number of detected ice floes has twin peaks, first in April and second in June, with the second likely indicating landfast ice breakup. The slope of the FSD steepens from April to late July, tracking the change in MIZ fraction. The steepening FSD slope indicates a relatively higher fraction of small floes versus large floes as the melt season progresses.

a Floe count — Median, 25-75%, 1-90%
b Total sea ice and MIZ extents
c Power law slope — Individual images, Binned by day of year

Measures of seasonal and interannual variability of the FSD. (a) Number of floes detected in scene by day of year. (b) Sea ice extent from the NSIDC Climate Data Record of Sea Ice Concentration in the study region. Top: area of grid cells with SIC > 15% in the study region. Bottom: Fraction of the sea ice extent with SIC between 15 and 85%. (c) Slope of the truncated power law for individual images (blue dots) and aggregated across all years by DOY (red dots). Box-and-whiskers show distribution of individual image estimates.

Future directions
These results show the capability of the IFT for assessing variability of the FSD. We have extended the prototype version of the IFT used here into a new, open-source implementation of the IFT pipeline using Julia and Python, enabling efficient application of the algorithm over much broader regions. We expect to release an expanded, updated version of the IFT dataset during Summer 2025. We see potential for using these floe-scale observations for the following:

- **Assessing spatial and temporal variation in FSD properties across the Arctic**
- **Relating variability in the FSD with sea ice dynamics**
- **Validating FSD parameterization in sea ice models**

IceFloeTracker.jl
Registered Julia software package for optical satellite image processing, sea ice segmentation, feature extraction, and ice floe tracking. Source code and example Jupyter notebooks available on GitHub.

The IFT Fram Strait Dataset
Processed MODIS satellite imagery, floe properties, and trajectories archived at the Brown Digital Repository.

References

[1] Squire, V. A. (2022). A prognostative synopsis of contemporary marginal ice zone research. *Philosophical Transactions of the Royal Society A: Mathematical, Physical and Engineering Sciences*, 380(2235), 20220094.

[2] Brenner, et al., (2023). Scale-Dependent Air-Sea Exchange in the Polar Oceans: Floe-Floe and Floe-Flow Coupling in the Generation of Ice-Ocean Boundary Layer Turbulence. *Geophysical Research Letters*, 50(23), e2023GL105703.

[3] Kim et al., (2025). Characterization of sea ice kinematics over oceanic eddies. *Journal of Fluid Mechanics* (in press)

[4] Lopez-Acosta et al., (2019). Ice Floe Tracker: An algorithm to automatically retrieve Lagrangian trajectories via feature matching from moderate-resolution visual imagery. *Remote Sensing of Environment*, 234(111406), pp1–15.

[5] Manucharyan et al. (2022a). Spinning ice floes reveal intensification of mesoscale eddies in the western Arctic ocean. *Scientific Reports*, 12(7070).

[6] Lopez-Acosta (2021). Sea Ice Drift in Arctic Marginal Ice Zones Derived from Optical Satellite Imagery [PhD Thesis]. University of California Riverside.

[7] Watkins et al., (2023). Evidence of abrupt changes in sea ice dynamics in the East Greenland marginal ice zone. *Geophysical Research Letters*, 50, e2023GL103558

[8] Lopez-Acosta et al. (2024). Fram Strait sea ice floe segmentation and tracking from moderate-resolution optical imagery (Version 0.1) [Dataset]. Brown Repository.

[9] Hatcher, S., Ahmed, A., Kim, M., & Wilhelmus, M. M. (2022). SOIT: Satellite overpass identification tool [Computer software]. Zenodo.

[10] Hwang et al., (2017). Winter-to-summer transition of Arctic sea ice breakup and floe size distribution in the Beaufort Sea. *Elementa: Science of the Anthropocene*, 5, 40.

[11] Buckley et al., (2024). Seasonal evolution of the sea ice floe size distribution in the Beaufort Sea from 2 decades of MODIS data. *The Cryosphere*, 18(11), 5031–5043.

[12] Clauset, Aaron, Cosma Rohilla Shalizi, and M. E. J. Newman. "Power-Law Distributions in Empirical Data." *SIAM Review* 51, no. 4 (November 4, 2009): 661–703.

[13] Alstott et al., (2014). powerlaw: A Python Package for Analysis of Heavy-Tailed Distributions. *PLoS ONE*, 9(1), e85777.

[14] Watkins et al., (2024). Observing floe-scale sea ice motion in the Greenland Sea marginal ice zone during summer. *Earth and Space Science Open Archive* [Preprint].